Applied Catalysis B: Environmental 84 (2008) 734–741

Contents lists available at ScienceDirect

Applied Catalysis B: Environmental

journal homepage: www.elsevier.com/locate/apcatb

Highly active and stable bimetallic Ir/Fe-USY catalysts for direct and NO-assisted N_2O decomposition

Qun Shen[a], Landong Li[a], Zhengping Hao[a,*], Zhi Ping Xu[b,**]

[a] Research Center for Eco-Environmental Sciences, Chinese Academy of Sciences, Beijing 100085, PR China
[b] Australian Research Council (ARC) Centre of Excellence for Functional Nanomaterials, Australian Institute for Bioengineering and Nanotechnology and School of Engineering, The University of Queensland, Brisbane, QLD 4072, Australia

ARTICLE INFO

Article history:
Received 18 January 2008
Received in revised form 26 March 2008
Accepted 22 May 2008
Available online 11 June 2008

Keywords:
Bimetallic catalyst
Ir/Fe-USY
Synergy
NO-assisted N_2O decomposition
Durability

ABSTRACT

The current research investigated N_2O decompositions over the catalysts Ir/Fe-USY, Fe-USY and Ir-USY under various conditions, and found that a trace amount of iridium (0.1 wt%) incorporated into Fe-USY significantly enhanced N_2O decomposition activity. The decomposition of N_2O over this catalyst (Ir/Fe-USY-0.1%) was also partly assisted by NO present in the gas mixture, in contrast to the negative effect of NO over noble metal catalysts. Moreover, Ir/Fe-USY-0.1% can decompose more than 90% at 400 °C (i.e. the normal exhaust temperature) under simulated conditions of a typical nitric acid plant, e.g. 5000 ppm N_2O, 5% O_2, 700 ppm NO and 2% H_2O in balance He, and such an activity can be kept for over 110 h under these strict conditions. The excellent properties of bimetallic Ir/Fe-USY-0.1% catalyst are presumably related to the good dispersion of Fe and Ir on the zeolite framework, the formation of framework Al–O–Fe species and the electronic synergy between the Ir and Fe sites. The reaction mechanism for N_2O decomposition has been further discussed on the temperature-programmed desorption profiles of O_2, N_2 and NO_2.

1. Introduction

N_2O (nitrous oxide), although present at relatively low concentrations in the troposphere, contributes significantly to global warming due to its 310-time damaging potential with respect to CO_2. Meanwhile, nitrous oxide severely destructs the ozone layer and also leads to the formation of acid rain [1]. Due to the negative effects on the global environment, nitrous oxide needs to be eliminated from the emissions of human activities. To this end, a direct and efficient method is to catalytically decompose N_2O to environmentally benign N_2 and O_2 prior to its emission to the air. However, the temperature of the tail-gas emission is not high enough to complete N_2O decomposition. Therefore, cost-effective catalysts that can efficiently decompose N_2O at moderate temperatures below 500 °C are urgently required and have been greatly researched in recent decades [2].

In search for effective catalysts, many kinds of materials, such as metal oxides or composites [3], Fe-exchanged zeolites (FER, Beta, MFI) [4–9], transition metal doped mesoporous materials (MCM-41, SBA-15) [10,11], and noble metals loaded on various supports [12,13] have been examined to catalytically decompose N_2O. Among these catalysts, noble metals supported on zeolites can efficiently decompose N_2O at the temperatures of 250–350 °C [12]. Unfortunately, N_2O decomposition over these supported noble metals is severely inhibited by the presence of NO [2], which is usually an unavoidable component in the tail-gas effluent emitted from, e.g. the nitric acid plant. Good news is that many transition metal-exchanged zeolites show moderate activity for N_2O decomposition in the temperature range of 450–600 °C [4–6,8,9,14–22] and that N_2O decomposition over iron-zeolites is strongly promoted by trace NO in the feed gas [16,17]. Moreover, some Fe-zeolites [8,9,14,22], such as Fe-ZSM-5 reported by Nam and coworkers [8] and Fe-USY we examined recently [22], exhibit remarkable stability under a simulated exhaust emission from a typical nitric acid plant. Therefore, combining both the merits of noble metal-zeolites and iron-zeolites motivated us to develop highly active NO-assisted bimetallic zeolite catalysts. In this work, we considered our previous observation that Fe-USY prepared via a simple wet ion-exchange method shows high activity and good durability for N_2O decomposition [21,22], and introduced iridium into the zeolites to examine its performance in N_2O decomposition. We have found that incorporating a trace amount of iridium

* Corresponding author. Tel.: +86 10 62849194; fax: +86 10 62923564.
** Corresponding author. Tel.: +61 7 33463809; fax: +61 7 33463973.
E-mail addresses: zpinghao@rcees.ac.cn (H. Zhengping), gordonxu@uq.edu.au (X. Zhi Ping).

0926-3373/$ – see front matter © 2008 Elsevier B.V. All rights reserved.
doi:10.1016/j.apcatb.2008.05.026

(0.1 wt%) into Fe-USY catalysts significantly enhances the catalytic activity and that the presence of NO can moderately assist N_2O decomposition. In comparison with some noble metal/Fe(Co)-zeolites reported elsewhere [18–20], our catalyst is more active, but with a much lower noble metal loading.

2. Experimental

2.1. Catalyst preparation

Commercial ultra-stable Y (USY, Si/Al = 11.6, specific surface area = 512.4 m^2/g) was provided by Sinopec Co. and directly used as the parent zeolite in this study. The parent zeolite (*ca.* 5 g) was added into 500 mL of 0.05 M $FeCl_3$ aqueous solution, and the ion exchange was carried out under vigorous stirring for 48 h at room temperature. Following ion exchange, the zeolite was filtered, thoroughly washed with deionized water, dried at 100 °C overnight and then calcined at 600 °C for 4 h in air. The Fe-loading USY was further treated by 0.01 M HCl aqueous solution for 6 h. After acid treatment, the Fe-zeolite was collected by filtration, washed with deionized water and dried at 100 °C overnight. Finally, the Fe-zeolite was calcined at 600 °C for 4 h and denoted as Fe-USY.

Ir/Fe-USY and Ir-USY were prepared from Fe-USY and H-USY, respectively, as follows. In a typical experiment, 2.0 g Fe-USY or H-USY was mixed with 10 mL $H_2IrCl_6{\cdot}6H_2O$ aqueous solution containing a desired amount of iridium. The water was evaporated in a vacuum at 60 °C and the residual solid was dried at 100 °C overnight. The dried sample was then calcined at 600 °C for 4 h and denoted as Ir/Fe-USY-*x*% or Ir-USY-*x*%, where *x* is the nominal mass percentage of Ir from 0.1 to 2.

2.2. Material characterizations

The Fe and Ir contents in these USY zeolites were determined by ICP-AES using an Optima 2000 spectrometer. Low temperature N_2 adsorption/desorption experiments were carried out in a Quantachrome NOVA-1200 gas absorption analyzer after heat treatment at 200 °C for 4 h in N_2 stream, and the specific surface area was calculated using the BET equation.

Temperature-programmed reduction (TPR) experiments were conducted in a conventional TPR apparatus using 8% H_2/He as the reducing agent at a heating rate of 10 °C/min from 100 to 800 °C. Prior to the reduction, the zeolite catalyst (100 mg) was pretreated at 500 °C in He for 2 h. The H_2 consumption was monitored online by a gas chromatograph equipped with a TCD detector.

Temperature-programmed desorption of O_2 (O_2-TPD) was carried out in a fixed-bed flow microreactor. The zeolite catalyst (200 mg) was pretreated in pure oxygen at 600 °C for 1 h and then cooled down to 100 °C in an O_2 stream (50 mL/min). The sample was further treated by flowing He for 4 h (50 mL/min) to remove the physically adsorbed oxygen on the catalyst surface. The sample was then heated to 600 °C at a heating rate of 5 °C/min in He, NO/He or NO_2/He (2500 ppm NO or NO_2, 50 mL/min) to examine desorption of O_2 and other species temporarily formed (if any) that was analyzed online by a quadrapole mass spectrometer (Agilent, 5973). Temperature-programmed desorption of N_2O (N_2O-TPD) and NO_2 (NO_2-TPD) was performed in a similar way, except that the sample was pretreated at 300 °C and cooled down in N_2O/He mixed stream (2% N_2O, 50 mL/min) where the desorbed O_2 and N_2 were also monitored online by the mass spectrometer.

2.3. Catalyst evaluation

N_2O decomposition experiments were performed in a fixed-bed flow microreactor at atmospheric pressure. In each run, 0.1 g catalyst (0.25–0.5 mm sieve fraction) was placed into a quartz reactor (4 mm i.d.) and pretreated in He at 600 °C for 1 h. After the reactor was cooled to 200 °C, the reactant gas mixture (N_2O, or O_2 or NO, He balance) was fed into the reactor. The total flow rate of the inlet gas was kept at 60 mL/min (corresponding GHSV = 30,000 h^{-1}). The outlet gas composition was analyzed online using a gas chromatograph (Agilent 6820 series) equipped with a TCD detector and two serial columns (a Porapak Q column served for the separation of N_2O and N_2/O_2, and a molecular sieve 5A column for the separation of N_2 and O_2). Steady-state activity data were recorded at 25 °C intervals at ascending temperature from 200 to 600 °C (for the activity test) and at some selected temperatures (for the durability test).

Assuming that N_2O decomposition is a first-order reaction, the rate of N_2O decomposition can be expressed as:

$$r = kP_{N_2O} = A\,e^{-E_a/RT}P_{N_2O}$$

The pseudo-first-order rate constant k was calculated using the formula:

$$k = \frac{-\mathrm{Ln}(1-x)F}{m_{cat}P}$$

where F is the total flow, m_{cat} is mass of the catalyst, P is the total pressure, and x is the N_2O conversion. The plot of $\ln(k)$ versus $1/T$ can thus give the apparent activation energy (E_a), and the associated pre-exponential factor (A).

3. Results and discussion

3.1. Physical characterization of zeolite catalysts

As listed in Table 1, the specific surface area of all Fe-USY and Ir/Fe-USY catalysts is very similar (535–554 m^2/g) and the total pore volume is close to one another (0.42–0.45 cm^3/g), so the iridium addition (0.1–2%) into Fe-USY does not change the textural properties of Fe-USY. This is because the structure of the USY zeolite is well preserved after iridium loading and subsequent calcination, as demonstrated by the XRD patterns (Fig. 1). Note that the determined Fe loading is very similar in these zeolites (2.05–2.10%) and that Ir loading is almost the same as the desired value, indicating the well-controlled deposition of Ir to Fe-USY in the experiments.

Fig. 2 displays the H_2-TPR profiles of Fe-USY, Ir-USY-0.1% and Ir/Fe-USY-0.1%. For the Ir-USY-0.1% sample, two weak peaks at about

Table 1
Textual properties of samples

Sample	S_{BET} (m^2/g)	Total pore volume (cm^3/g)	Fe loading (wt%)	Ir loading (wt%)
Fe-USY	536	0.43	2.10	/
Ir/Fe-USY-0.1%	550	0.44	2.08	0.09
Ir/Fe-USY-0.5%	554	0.45	2.05	0.49
Ir/Fe-USY-1%	540	0.43	2.07	0.98
Ir/Fe-USY-2%	535	0.42	2.05	1.99

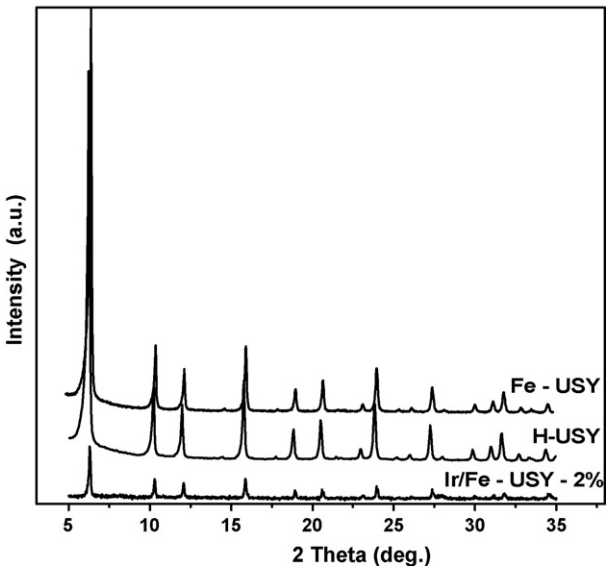

Fig. 1. XRD patterns of H-USY, Fe-USY, Ir/Fe-USY-2%.

260 and 290 °C were observed, presumably ascribed to the reduction of iridium oxide [23]. For the Fe-USY sample, two strong peaks centered at 360 and 440 °C were observed, attributed to the reduction of various Fe(III) to Fe(II) ions (isolated ions, clusters and nanoparticles) in USY [7,24–26]. In addition, there is no obvious reduction peak from 500 to 700 °C, which corresponds to the reduction of FeO to Fe^0 in the nanoparticle form [7,15] and suggests that there are fewer Fe_2O_3 nanoparticles in the zeolite, if any. Incorporation of Ir into Fe-USY (Ir/Fe-USY-0.1%) results in two reduction peaks at 286 and 380 °C, compromising the reduction of Ir^{4+} to Ir^0 and Fe(III) to Fe(II). The change in position and shape of the H_2 reduction signals might reflect synergic interactions between Fe and Ir. Other factors might also play a role, such as sitting of Ir and Fe in the cages of zeolite Y, interactions of Fe and Ir with Al (extra-lattice or in the lattice) and so on.

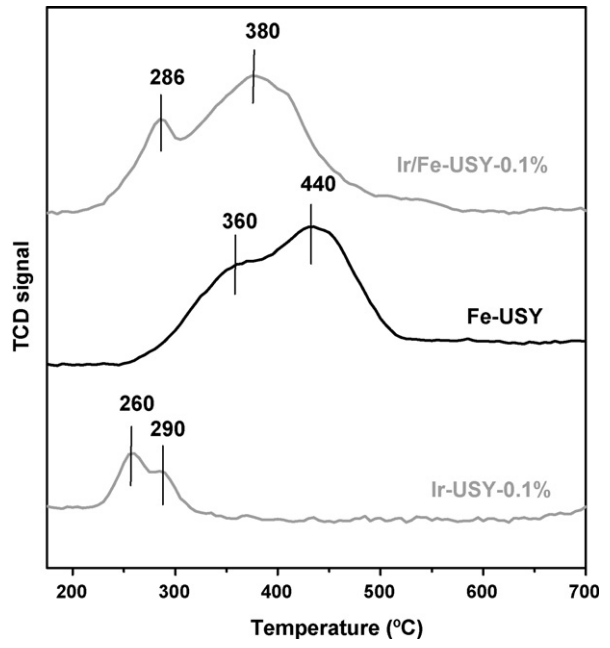

Fig. 2. H_2-TPR profiles of Ir-USY-0.1%, Fe-USY and Ir/Fe-USY-0.1%.

3.2. Catalytic performances

Fig. 3A shows that Ir-USY catalysts have a much higher activity than Fe-USY for N_2O decomposition. Even though Ir-USY-0.1% catalyst contains only 0.1 wt% Ir, the catalytic performance is much better than Fe-USY (with 2.10 wt% Fe). Note that the catalytic activities of the Ir-USY-*x*% catalysts strongly depend on the iridium loading. In general, the higher the Ir loading, the higher the activity. In the case of Ir-USY-2%, 100% N_2O conversion occurred at 375 °C, which is similar to the results of Li and Armor [12] and Oi et al. [13] for noble metal catalysts.

The catalytic performance of Ir/Fe-USY-*x*% catalysts (Fig. 3B) indicates that the addition of iridium significantly improves the catalytic activity in comparison with Fe-USY. For example, the temperatures for 50% and 100% N_2O conversion over Ir/Fe-USY-*x*% are 50–100 °C lower than over Fe-USY catalyst. When compared with Ir-USY-*x*% with the same Ir loading, catalysts Ir/Fe-USY-0.5%, -1% and -2% demonstrate similar activity (comparing Fig. 3A with B). In sharp contrast, catalyst Ir/Fe-USY-0.1% shows remarkable improvement in catalytic activity, compared with both Fe-USY and Ir-USY-0.1%. More surprisingly, Ir/Fe-USY-0.1% gives a higher N_2O conversion than Ir/Fe-USY-2.0% below 320 °C (Fig. 3B). The higher activity of Ir/Fe-USY-0.1% is speculatively ascribed to the synergic effect between iridium and iron oxide on the zeolite framework, as suggested by their H_2-TPR profiles (Fig. 2). It is worth noting that zeolite supported bimetallic catalysts, such as Ru/Fe-FER [18] and Pt/Fe-FER [19], have been reported as very good catalysts for N_2O decomposition. However, Fig. 3C shows that these catalysts, i.e. Ru/Fe-USY-0.1%, Rh/Fe-USY-0.1% and Pd/Fe-USY-0.1%, prepared in the same way as Ir/Fe-USY-0.1% with the same weight loading (0.1 wt%), are less active than Ir/Fe-USY-0.1%. Moreover, the N_2O decomposition activity of Ir/Fe-USY-0.1% is comparable with, or even better than, the noble/transition bimetallic zeolite catalysts reported elsewhere [18–20]. Such a catalyst (Ir/Fe-USY-0.1%) that can be prepared by the simple method with a much lower noble metal loading but with a higher activity appears to be a promising catalyst candidate for future application.

In accordance with Pieterse's report that N_2O decomposition over supported noble metal catalysts was strongly inhibited by NO, O_2 and H_2O [2], we also observed that the presence of NO (700 ppm) or O_2 (5%) in feed gas has a somewhat negative effect on N_2O decomposition over Ir-USY-2% (data is not shown here). The same phenomenon also occurred on the other Ir-USY-*x*% catalysts. The negative effect of NO and O_2 is normally attributed to their competitive adsorption on the active Ir sites against N_2O, as suggested by Pirngruber for supported Ru catalyst [2]. In contrast, other reports [4,22] show that NO assists N_2O decomposition over Fe-zeolite catalysts while the presence of O_2 still has a negative effect. Thus it is of interest to know what the effect on N_2O decomposition will be when NO is present in the stream over Ir/Fe-USY-*x*% catalysts. As shown in Fig. 4A and B, O_2 always inhibits N_2O decomposition for both Ir/Fe-USY-0.1% and -2%. Interestingly, NO assists N_2O decomposition over catalyst Ir/Fe-USY-0.1% (especially at the high N_2O conversion) but have limited effect over catalyst Ir/Fe-USY-2%. We ascribe the NO assistance over Ir/Fe-USY-0.1% to the dominance of Fe's promotion and the limited effect to the trade-off between Fe's promotion and Ir's prohibition. The different effect of NO on N_2O decomposition over Ir/Fe-USY-0.1% and Ir/Fe-USY-2% may suggest different decomposition pathways over these two catalysts.

Based on the assumption of first-order reaction, the apparent activation energy (E_a) and the associated pre-exponential factor (A) for N_2O decomposition on different catalysts under different conditions were calculated, as listed in Table 2. The apparent activation energy (E_a) of N_2O decomposition on Ir/Fe-USY-0.1% is

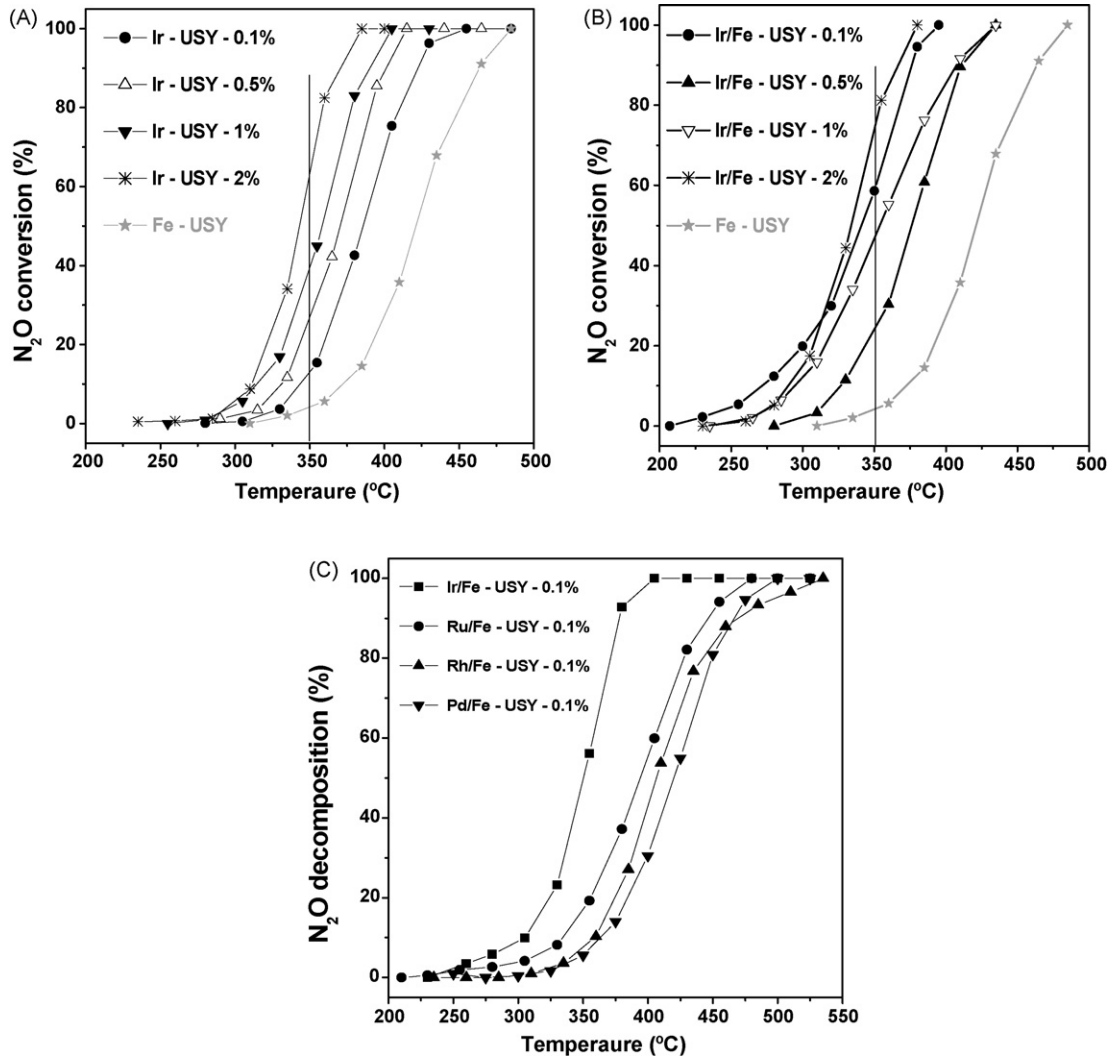

Fig. 3. (A) and (B) Steady-state N_2O conversion over catalysts Fe-USY, Ir-USY-*x*% and Ir/Fe-USY-*x*% vs. temperature; (C) steady-state N_2O conversion over different noble metal modified Fe-USY conditions of 0.1 g catalyst, 5000 ppm N_2O and balance He with flowing rate of 60 mL/min, GHSV = 30,000 h^{-1}.

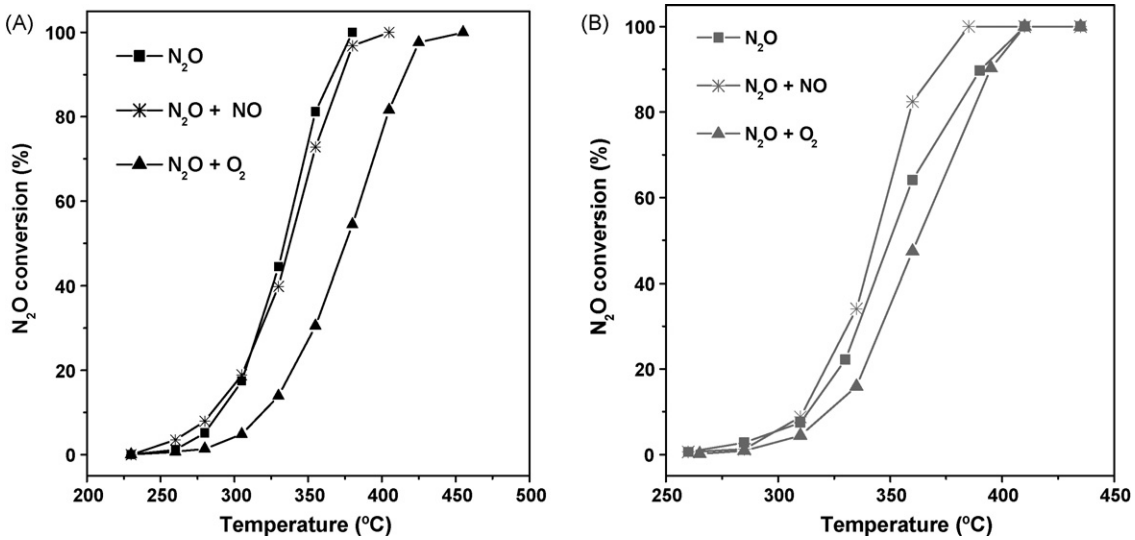

Fig. 4. (A) and (B) Effect of O_2 and NO in the stream on N_2O conversion over catalysts Ir/Fe-USY-2% and Ir/Fe-USY-0.1% under conditions of 0.1 g catalyst, 5000 ppm N_2O, 0 or 5% O_2, 0 or 700 ppm NO, in balance He with the flowing rate of 60 mL/min, i.e. GHSV = 30,000 h^{-1}.

Table 2
Calculated apparent activation energy and pre-exponential factor for N_2O decomposition on different catalysts under different reaction conditions

Sample	Mixed gases in He	E_a (kJ/mol)	A ($mol_{N_2O}/S\,g_{cat}\,Pa_{N_2O}$)
Fe-USY	5000 ppm N_2O	139	16.4
Fe-USY	5000 ppm N_2O + 700 ppm NO	100	8.2×10^{-2}
Fe-USY	5000 ppm N_2O + 5% O_2	141	24.5
Ir-USY-0.1%	5000 ppm N_2O	157	1.6×10^{3}
Ir-USY-0.1%	5000 ppm N_2O + 700 ppm NO	138	24.5
Ir-USY-0.1%	5000 ppm N_2O + 5% O_2	164	1.6×10^{3}
Ir/Fe-USY-0.1%	5000 ppm N_2O	85.6	1.4×10^{-2}
Ir/Fe-USY-0.1%	5000 ppm N_2O + 700 ppm NO	80.1	6.7×10^{-3}
Ir/Fe-USY-0.1%	5000 ppm N_2O + 5% O_2	119	5.5

much lower than Ir-USY-0.1% and Fe-USY under the same conditions. Note that the addition of 700 ppm NO in the feed gas reduces the activation energy while excess oxygen (5%) increases the activation energy over all catalysts. In particular, the activation energy of 85.6 and 80.1 kJ/mol over Ir/Fe-USY-0.1% is the lowest for direct and NO-assisted N_2O decomposition, respectively, in all cases.

A good catalyst for practical application requires not only higher activity but also longer durability. Therefore, we further tested the durability of Ir/Fe-USY-0.1% catalyst under simulated conditions of a typical nitric acid plant, i.e. 5000 ppm N_2O, 5% O_2, 700 ppm NO and 2% H_2O (balance He) in the stream. The time-on-stream profile of Ir/Fe-USY-0.1% in Fig. 5 shows that there is no obvious activity loss for 110 h at 325, 350 or 400 °C. This indicates that the catalyst is highly durable under these conditions. The good durability of Ir/Fe-USY-0.1%, like Fe-USY, could be attributed to the high degree of exchange (high Fe loading) and the formation of framework Al–O–Fe species that stops the dealumination from the zeolite framework and subsequent clustering of iron species [22]. Such a property makes this catalyst more attractive in the potential application.

3.3. Investigation of N_2O decomposition mechanism

In regard to the N_2O decomposition mechanism, different reaction pathways have been proposed [27–31]. In general, N_2O chemisorption first takes place on the active site of the catalyst, followed by the N_2 release and the formation of chemisorbed oxygen on the active site (R1). The chemisorbed oxygen can then be desorbed as O_2 (rate determining step) via Langmuir–Hinshelwood mechanism (R2) and/or Eley–Rideal mechanism (R3), and the active site is regenerated.

$$N_2O + * \xrightarrow{k1} N_2 + {}^{*}\!-O \quad \text{(R1)}$$

$$2{}^{*}\!-O \xrightarrow{k2} O_2 + 2* \quad \text{(R2)}$$

$$N_2O + {}^{*}\!-O \xrightarrow{k3} N_2 + O_2 + * \quad \text{(R3)}$$

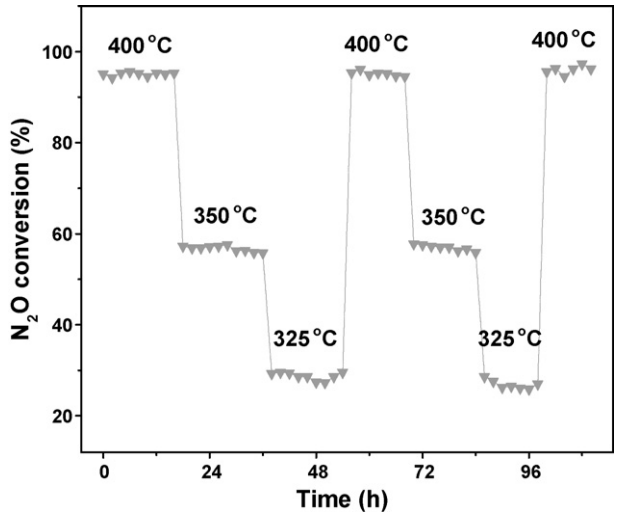

Fig. 5. Time-on-stream behavior of Ir/Fe-USY-0.1% catalyst for the decomposition of N_2O at different temperatures under conditions of 0.25 g catalyst, 5000 ppm N_2O, 5% O_2, 700 ppm NO and 2% H_2O in balance He at the flow rate = 60 mL/min and GHSV = 30,000 h^{-1}.

To verify such decomposition pathways and to reveal the effects of experimental conditions, a series of TPD experiments were conducted. First of all, we recorded the O_2-TPD profiles from Fe-USY, Ir-USY-0.1% and Ir/Fe-USY-0.1% catalysts (Fig. 6A–C), illustrating the Ir effect on oxygen desorption behavior. For the Fe-USY catalyst, oxygen desorption starts at 400 °C, takes place significantly at 450 °C and reaches the maximum at 540 °C (Fig. 6A). In the experiment, we noted that 25% N_2O is decomposed at 400 °C (Fig. 3B). This suggests that it is very likely for chemisorbed oxygen to desorb according to (R3) at low temperatures, i.e. gaseous N_2O takes part in the chemisorbed oxygen desorption. Reaction (R2) may start at temperatures above 400 °C.

For Ir-USY-0.1%, chemisorbed oxygen desorption begins at about 300 °C, occurs obviously at 350 °C and reaches the maximum at 480 °C (Fig. 6B), which is coincident to N_2O decomposition where N_2O starts to decompose at 300 °C and completely decomposes at 475 °C (Fig. 3A). Thus the chemisorbed oxygen on Ir-USY-0.1% could be removed by recombining two chemisorbed oxygens (R2) and/or reacting with gaseous N_2O (R3). For Ir/Fe-USY-0.1%, oxygen desorption starts at 300 °C and is obvious at 400 °C, but there is no maximum until 600 °C (Fig. 6C). However, the N_2O decomposition is already obvious (20% conversion) at 300 °C. This observation suggests that the chemisorbed oxygen on Ir/Fe-USY-0.1% catalyst could mostly be removed via the Eley–Rideal mechanism (R3) at low temperatures, similar to Fe-USY. Careful comparison indicates that oxygen desorption mainly undergoes (R3) as N_2O decomposition at 375 °C is almost completed (Fig. 3B), while the chemisorbed oxygen desorbs to a less extent (Fig. 6C). Therefore, Ir in Ir/Fe-USY-0.1% can facilitate direct desorption of chemisorbed oxygen, but to a limited degree, compared with Fe-USY, and moreover, the higher activity of catalyst Ir/Fe-USY-0.1% could be attributed to reaction (R3) by consuming the chemisorbed oxygen and leave the active sites.

The N_2O-TPD profile on Ir/Fe-USY-0.1% sample is displayed in Fig. 6D. During the whole desorption process, N_2O is not monitored in the outlet stream while N_2 and O_2 are detected. The desorption products suggest that the adsorbed N_2O is readily dissociated into chemisorbed N_2 and O_2 on the catalyst surface at 300 °C during the pre-treatment. Note that N_2 is detected below 200 °C, lower than

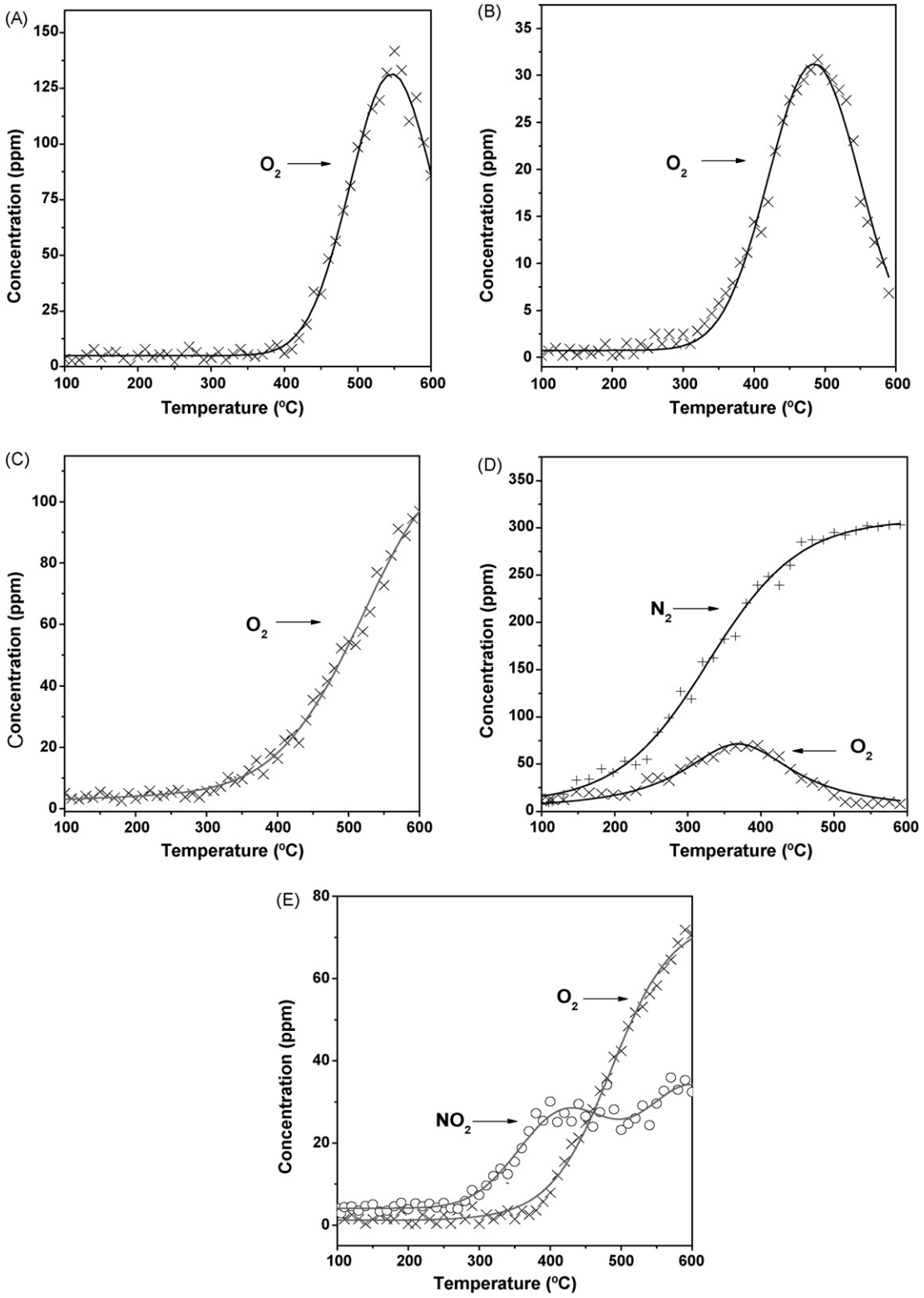

Fig. 6. (A) O_2-TPD in He over Fe-USY; (B) O_2-TPD in He over Ir-USY-0.1%; (C) O_2-TPD in He over Ir/Fe-USY-0.1%; (D) N_2O-TPD in He over Ir/Fe-USY-0.1%; (E) O_2-TPD in 1% NO/He over Ir/Fe-USY-0.1%.

the N_2O decomposition temperature. This reveals that N_2 is weakly adsorbed and its desorption is easier than O_2 with low activation energy, as reported by Yakovlev et al. [32]. More interestingly, the desorbed N_2 amount is greater than O_2, i.e. the ratio N_2/O_2 at every temperature point is greater than the stoichiometric ratio (2). Therefore, the rate-determining step for N_2O decomposition is desorption of chemisorbed oxygen rather than chemisorbed nitrogen [33].

The presence of oxygen in the gas stream inhibits N_2O decomposition, because the chemisorption of oxygen on the

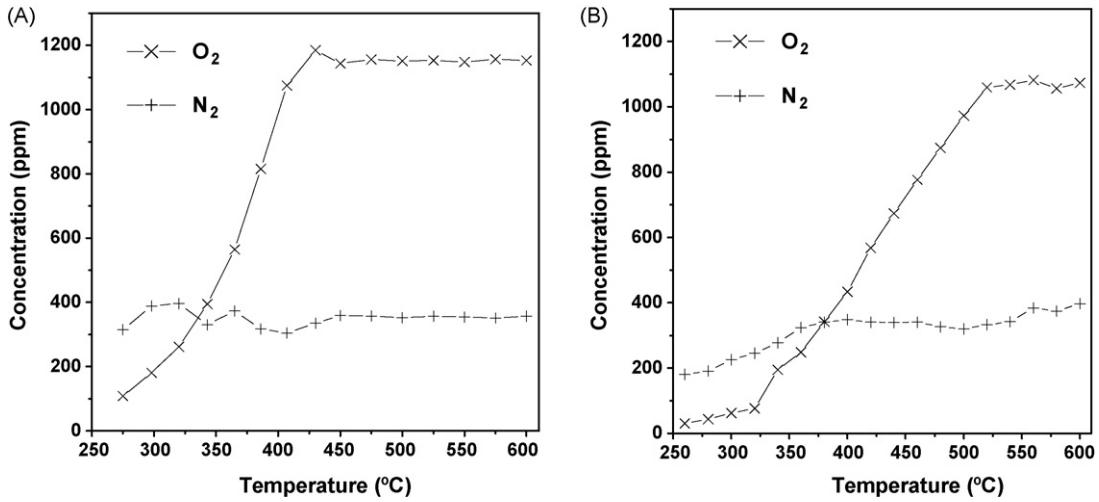

Fig. 7. Temperature-programmed reaction with flowing 2500 ppm NO_2/He over Ir/Fe-USY-0.1% (A) and Fe-USY (B) at heating rate = 5 °C/min from 250 to 600 °C.

catalytic active site, as expressed in (R4) (reverse reaction of (R2)), decreases the number of active sites and inhibits the chemisorption of N_2O (R1).

$$O_2 + * \xrightarrow{k4} {}^{*}{-}O_2; \qquad {}^{*}{-}O_2 + * \xrightarrow{\text{fast}} 2{}^{*}{-}O \tag{R4}$$

We also noted that NO shows a considerable promotion effect on N_2O decomposition over Ir/Fe-USY-0.1% (Fig. 4B). When the chemisorbed oxygen was desorbed in NO/He mixture gas (Fig. 6E) rather than in pure He (Fig. 6C), significantly less oxygen gas was detected at 300–400 °C but some NO_2 was simultaneously detected. This event reveals that some chemisorbed oxygen reacts with gaseous NO and desorbs in NO_2 molecule, as schemed in reaction (R5).

$$NO + *{-}O \rightarrow *{-}NO_2; \qquad *{-}NO_2 \rightarrow * + NO_2 \tag{R5}$$

As NO_2 can desorb at temperatures as low as 100–300 °C (Fig. 6E), NO promotes the removal of chemisorbed oxygen in this way and speeds up N_2O decomposition. As proposed by Pirngruber et al. [2] and Sang et al. [34], the chemisorbed NO_2 can decompose via reaction (R6) and/or reaction (R7) to promote the decomposition of N_2O by releasing more active sites.

$$*{-}NO_2 + N_2O \rightarrow O_2 + N_2 + NO + * \tag{R6}$$

$$2 * {-}NO_2 \rightarrow 2 * + 2NO + O_2 \tag{R7}$$

As chemisorbed NO_2 is formed by NO oxidation over the catalyst, we further carried out the temperature-programmed reaction of NO_2 by flowing 2500 ppm NO_2/He over catalysts Ir/Fe-USY-0.1% and Fe-USY from 250 to 600 °C to further understand the reaction mechanism. As shown in Fig. 7A, the concentration of generated N_2 seems to be a constant from 250 to 600 °C, so the apparent decomposition NO_2 to N_2 and O_2 occurs, probably via (R8) and in a constant rate:

$$2 * {-}NO_2 \rightarrow 2 * {-}O + O_2 + N_2 \tag{R8}$$

In contrast, the concentration of O_2 quickly increases with the temperature increasing to 425–450 °C, indicating that reaction (R7) becomes more and more pronounced. However, the O_2 concentration is kept constant above 450 °C, revealing that the decomposition of NO_2 is probably complete, with $O_2/N_2 = 3$ (Fig. 7A). The behavior of the NO_2 reaction over Fe-USY is very similar, only at a higher temperature (Fig. 7B). So relatively, NO_2 prefers to directly decompose to N_2 and O_2 at lower temperatures (R8) but to NO and O_2 at higher temperatures (R7), and reaches a steady state above 425–450 °C. From this discussion, we can see that the NO-assisted N_2O decomposition is realized through oxidation with chemisorbed oxygen to NO_2, which significantly decomposes at temperatures (350–400 °C, Fig. 7) much lower than direct desorption of chemisorbed oxygen (450–600 °C, Fig. 6C).

The reactions of NO_2 over catalysts Ir/Fe-USY-0.1% and Fe-USY can also help explain the N_2O decomposition behavior in the presence of NO_2 (Fig. 8). The presence of NO_2 inhibits N_2O decomposition at lower temperatures (<370 °C) to some extent because of the competing adsorption on the active sites between NO_2 and N_2O. However, at higher temperatures (>370 °C), most adsorbed NO_2 is transferred to NO and O_2 (see in Fig. 7A) and the generated NO can help remove the chemisorbed oxygen, thus promoting N_2O decomposition. Adsorbed NO_2 decomposition (R7) was proposed by Pirngruber et al. to occur on Ru over Ru/Fe-FER catalyst [2]. However, this work indicates that NO_2 decomposition (R7) can also proceed on Fe-USY and the incorporation of iridium lowers the temperature for NO_2 decomposition (Fig. 7B).

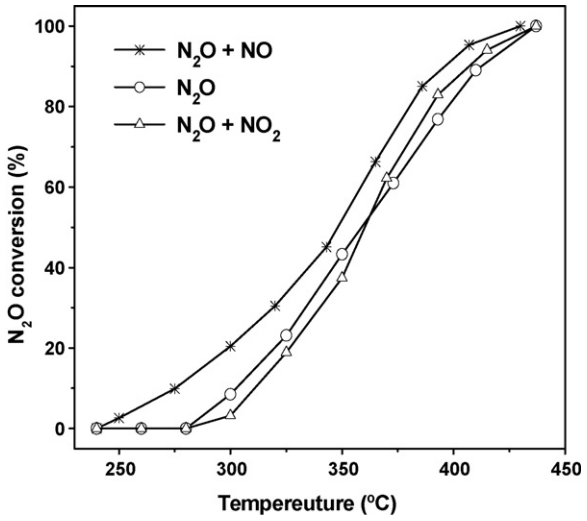

Fig. 8. Temperature-programmed reactions for N_2O decomposition over Ir/Fe-USY-0.1%. Reaction conditions were: 0.1 g catalyst, 5000 ppm N_2O, 0 or 700 ppm NO, 0 or 700 ppm NO_2, He balance flow rate = 60 mL/min and GHSV = 30,000 h^{-1}, heating rate = 5 °C/min.

In brief, the rate-determining step, i.e. desorption of chemisorbed oxygen in N_2O decomposition, could be mostly promoted via reaction (R3) (not (R2)) over Ir/Fe-USY-0.1%. NO in the reaction stream enhances desorption while the gaseous O_2 inhibits desorption of chemisorbed oxygen, i.e. having the opposite effect on N_2O decomposition over bimetallic Ir/Fe-USY-0.1% catalyst.

3.4. Synergic effect between iridium and iron

Zeolites supported noble metal/iron catalysts have been reported as promising catalysts for NO-assisted N_2O decomposition because of the synergy between noble metal and iron species [2,18,19]. For example, the catalytic synergy for N_2O decomposition over Ru/Fe-FER has been proposed by Pirngruber et al. [2] to be the major reason. They proposed that reactions (R5) (first half) and (R7) occur rapidly over Fe sites and Ru sites, respectively. However, the spillover of adsorbed NO_2 from Fe sites to Ru sites may be restricted by the low mobility. In this work, we have noted that all reactions ((R5)–(R8)) for NO-assisted N_2O decomposition can take place on Fe sites and we believe that the electron-transfer between iridium and iron-sites would be a significant synergic effect to enhance the activity although there is no direct experimental evidence.

Very interestingly, the synergic effect seems only observable in Ir/Fe-USY-0.1% catalyst, not in other ones (Ir wt% = 0.5–2), a bit different from the finding by Pirngruber et al. [2] that Ru/Fe-FER with 0.4 wt% Ru showed the synergic effect. The reason could be the segregation of Ir species at higher loadings so that the activity is mainly a compromise of the contributions of both Ir and Fe active sites.

4. Conclusion

In this research, we found that adding 0.1% iridium to Fe-USY (Ir/Fe-USY-0.1%) significantly enhances the N_2O decomposition activity in comparison with both Fe-USY and Ir-USY-0.1%. The positive effect of NO on N_2O decomposition over this catalyst presents a contrast to the negative effect normally observed for noble metal catalysts, including Ir-USY-*x*%. Ir/Fe-USY-0.1% also shows high stability for N_2O decomposition under the simulated conditions containing 5000 ppm N_2O, 5% O_2, 700 ppm NO and 2% H_2O with the balance being He at a typical nitric acid plant. These excellent properties of catalyst Ir/Fe-USY-0.1% could be attributed to the good dispersion of Fe and Ir on the zeolite framework, the formation of framework Al–O–Fe species [22] as well as the possible synergy between Ir and Fe sites, making this catalyst a cost-effective candidate for catalytic N_2O elimination. The investigation of the N_2O decomposition mechanism reveals that the incorporation of 0.1% Ir into Fe-USY reduces the activation energy for desorption of chemisorbed oxygens, the rate-determining step, and thus improves the catalytic performance.

Acknowledgements

This work was financially supported by National Natural Science Fund of China (20725723, 20703057) and National Basic Research Program of China (2004CB719500). The support from the ARC Centre of Excellence for Functional Nanomaterials funded by the Australia Research Council under its Centre of Excellence Scheme is also appreciated.

References

[1] J. Haber, T. Machej, J. Janas, M. Nattich, Catal. Today 90 (2004) 15.
[2] G.D. Pirngruber, L. Frunz, J.A.Z. Pieterse, J. Catal. 243 (2006) 340.
[3] N. Russo, D. Fino, G. Saracco, V. Specchia, Catal. Today 119 (2007) 228–232.
[4] R. Joyner, M.J. Stockenhuber, J. Phys. Chem. B 103 (1999) 5963.
[5] A. Wącław, K. Nowińska, W. Schwieger, A. Zielińska, Catal. Today 90 (2004) 21.
[6] J. Perez-Ramırez, J.C. Groen, A. Bruckner, M.S. Kumar, U. Bentrup, M.N. Debbagh, L.A. Villaescusa, J. Catal. 232 (2005) 318.
[7] A. Guzmán-Vargas, G. Delahay, B. Coq, Appl. Catal. B 42 (2003) 369.
[8] J.-H. Park, J.-H. Choung, I.-S. Nam, S.-W. Ham, Appl. Catal. B 78 (2008) 342.
[9] J.A.Z. Pieterse, G.D. Pirngruber, J.A. van Bokhoven, S. Booneveld, Appl. Catal. B 71 (2007) 16.
[10] X.D. Xu, H.L. Xu, F. Kapteijn, J.A. Moulijn, Appl. Catal. B 53 (2004) 265.
[11] S. Kawi, S.Y. Liu, S.-C. Shen, Catal. Today 68 (2001) 237.
[12] Y. Li, J.N. Armor, Appl. Catal. B 1 (1992) L21.
[13] J. Oi, A. Obuchi, G.R. Bamwenda, A. Ogata, H. Yagita, S. Kushiyama, K. Mizuno, Appl. Catal. B 12 (1997) 277.
[14] P. Marturano, L. Drozdová, G.D. Pirngruber, A. Kogelbauer, R. Prins, Phys. Chem. Chem. Phys. 3 (2001) 5585.
[15] J.A.Z. Pieterse, S. Booneveld, R.W. van den Brink, Appl. Catal. B 51 (2004) 215.
[16] G.D. Pirngruber, J.A.Z. Pieterse, J. Catal. 237 (2006) 237.
[17] G. Mul, J. Pérez-Ramírez, F. Kapteijn, J.A. Moulijn, Catal. Lett. 77 (2001) 7.
[18] J.A.Z. Pieterse, G. Mul, I. Melian-Cabrera, R.W. van den Brink, Catal. Lett. 99 (2005) 41.
[19] D. Kaucký, K. Jíša, A. Vondrová, J. Nováková, Z. Sobalík, J. Catal. 242 (2006) 270.
[20] Z. Sobalík, K. Jíša, D. Kaucký, A. Vondrová, Z. Tvarůžková, J. Novákova, Catal. Lett. 113 (2007) 124.
[21] L.D. Li, Z.P. Hao, J.J. Yu, Q. Shen, Chinese Patent 200610165546.8.
[22] L.D. Li, Q. Shen, J.J. Yu, Z.P. Hao, Z.P. Xu, G.Q. Max Lu, Environ. Sci. Technol. 41 (2007) 7901.
[23] H.J. Tian, T. Zhang, X.Y. Sun, D.B. Liang, L.W. Lin, Appl. Catal. A 210 (2001) 55.
[24] M. Yoshida, T. Nobukawa, S. Ito, K. Tomishige, K. Kunimori, J. Catal. 223 (2004) 454.
[25] T.V. Voskoboinikov, H.Y. Chen, W.M.H. Sachtler, Appl. Catal. B 19 (1998) 279.
[26] L.J. Lobree, I.C. Hwang, J.A. Reimer, A.T. Bell, J. Catal. 186 (1999) 242.
[27] F. Kapteijn, J. Rodriguez-Mirasol, J.A. Moulijn, Appl. Catal. B 9 (1996) 25.
[28] A. Vannice, T. Yamashita, J. Catal. 161 (1996) 254.
[29] E.V. Kondratenko, J. Pérez-Ramírez, J. Phys. Chem. B 110 (2006) 22586.
[30] N. Hansen, A. Heyden, A.T. Bell, F.J. Keil, J. Catal. 248 (2007) 213.
[31] S. Suarez, M. Yates, A.L. Petre, J.A. Martin, P. Avila, J. Blanco, Appl. Catal. B 64 (2006) 302.
[32] A.L. Yakovlev, G.M. Zhidomirovb, R.A. van Santen, Catal. Lett. 75 (2001) 45.
[33] D.A. Bulushev, A. Renken, L. Kiwi-Minsker, J. Phys. Chem. B 110 (2006) 10691.
[34] C. Sang, B.H. Kim, C.R.F. Lund, J. Phys. Chem. B 109 (2005) 2295.